Flow Studies of Mixed-Flow Compressor Impeller at Designed and Off-Design Condition

Vishal Doshi and Prof. Dinesh Kamble
Department of Mechanical Engineering (Heat Power)
Rajiv Gandhi Institute of Technology,
Mumbai, Maharashtra, India
vishalaero20@gmail.com
kambledinesh@gmail.com

Emandi Rajesh
Scientist, Propulsion Division
National Aerospace Laboratories
Bangalore, Karnataka, India
rajesh_emandi@nal.res.in

Abstract - High speed mixed-flow impeller has been designed for the Small Gas Turbine applications. Numerical Simulation has been carried out of a high blade loading main blade and the splitter blades for achieving the preliminary performance curves. CFD analysis has been carried out inorder to increase the performance and efficiency of the mixed-flow Impeller.

Internal flow irreversibility and Disk friction losses has been investigated at the Design point. Discharge mixing losses due to distorted flow (Jet and Wake) is absent at design point but can be captured at near choke condition. Choke margin can be improved by proper (t/c) distribution at the leading edge specifically near the pressure surface where flow reversal and normal shock is captured. Backsweep angle and cone angle modification would help to result into proper flow development near to choke condition.

Keywords: *Mixed-Flow Impeller, CFD analysis, Choke margin, Normal Shock, Stall.*

Nomenclature

C	***absolute velocity, m/s***
M	***Absolute Mach number***
Mrel	***Relative Mach number***
U	***Peripheral Velocity, m/s***
W	***Relative Velocity, m/s***
nf	***Number of Blades***
β	***Relative air angle, degrees***
α	***Absolute air angle, degrees***
η_{ts}	***Total-to-Static isentropic efficiency***
Ø	***Cone angle, degrees***
σ	***Slip Factor***

Subscripts

a	***axial***
b	***blade***
h	***Hub***
t	***tip***

Positions

1	***Inlet***
2	***Outlet***

*****

I. INTRODUCTION

Impellers with 762 m/s tip speeds; some with backward leaning blades has been designed. It has been the center of interest about knowing the performance of the mixed-flow compressor because it is well-known that the compressor efficiency has the strongest influence of fuel consumption out of any component in a Gas Turbine Engines.

For the case of mixed-flow compressor, two separate sources of work input can be seen as follows [3]:

$$\text{Work Done} = (U_2C_{t2} - U_1C_{t1}) + (U_2 - U_1) \qquad \text{[Eq. 1]}$$

$$= \begin{pmatrix} specific\ work\ input \\ due\ to \\ aerodynamic\ forces \end{pmatrix} + \begin{pmatrix} specific\ work\ input \\ due\ to \\ coriolis\ forces \end{pmatrix}$$

Energy must transfer efficiently from rotor to fluid in large measure by imposing meridional streamline radially outward shift. Annulus design for mixed-flow turbo-machines become as crucial to the specification of work input and enthalpy as the selection of blade profile shapes in case of axial machines.

Sr. No	Parameter	Values
1	Corrected mass flow rate (m_c)	1.742 kg/s
2	Corrected Speed (N_c)	50067 RPM
3	Total-to-total Pressure ratio (π_c)	6:1
4	Prewhirl	0˚

Table. 1 Design Parameters for Mixed-Flow rotor

The large concern is for the efficiency with which the work input process is accomplished. In general, an impeller suffers three kinds of losses which will be investigated in the present work [3].

- Disk and cover (or shroud) friction
- Internal flow irreversibilities and
- Discharge mixing losses engendered by a distorted flow leaving the impeller.

II. NUMERICAL SIMULATION

Numerical simulation was carried out using commercial code ANSYS CFX 15.0 and mesh was generated using Turbo grid. A fluid zone body cut into sector using periodic surface consists of one main blade and one splitter blade has been generated in Bladegen. 11 main blades and 11 splitter blades (50% of main blade length) has been used for the present work.

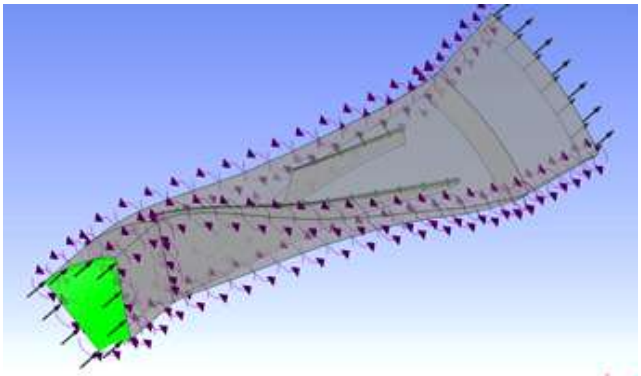

Figure.1 Control volume passage of a sector (one main blade and one splitter blade)

A. Turbulence Model:

For the present work the Shear Stress Transport (SST) turbulence model is used to overcome the shortcomings of the k-ϵ and k-ω models. The SST model is a blended two-equation model combining the above tow mentioned turbulence models. k-ω model near the wall and transitions to k-ϵ model away from the wall. Thus, it takes advantage of the superior performance and accuracy of the k-ω in the near wall regions, and avoids the free stream sensitivity of the ω equation by replacing it with the k-ϵ equation in the far field.

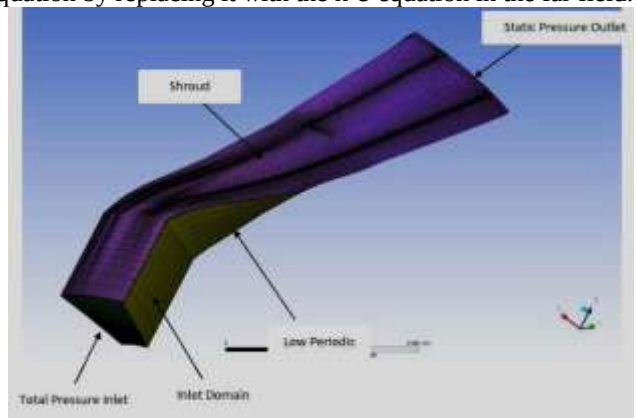

Figure. 2 Meshed model with Hexahedral Element

B. Topology Setup :

Traditional H/J/C/L-Grid is selected for the present work. H/J/C/L-Grid allows a separate choice of topology type for the upstream and downstream end of the passage mesh. The topology mesh is been optimized with the help of O-Grid, having width factor of 0.4 to adjust the thickness between them. Periodicity is given to the topology to reduce the CPU run time.

C. Grid Independency Test :

Hexahedral element with y+ method has been used for meshing for the present work. Value of y+ less than one is maintained near the hub and shroud surface. Grid dependency study was carried out with mesh size of 0.96 million and 1.46 million number of nodes. The change in Total-to-Static pressure and isentropic efficiency with respected to mass flow rate parameter shows less than 2% [Fig.3]. Thus mesh size of 1.46 million has been used which shows comparatively accurate results near to stall point.

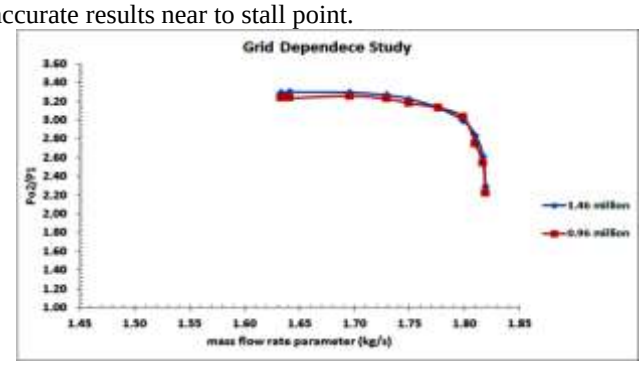

Figure 3 Grid Dependency Test

III BOUNDARY CONDITIONS

Total Pressure and Total Temperature with 5% intensity and eddy viscosity ratio turbulence is used as boundary condition at inlet. Average Static Pressure with pressure profile bend of 0.05 is used as boundary condition at Outlet. Hub surface and Shroud surface are given wall with no slip condition as boundary conditions with frame type as rotating and counter-rotating respectively. Wall roughness is kept smooth with adiabatic heat transfer condition. RMS residual type is selected with the convergence criteria of 1e-6 is set.

Parameters	Values
t_h	0.0015m
t_t	0.0010m
β_{1t}	61˚
β_{1h}	36.7˚
β_{2b}	-25˚
d_{2t}	189mm
ϕ_2	32˚
α_2	72˚

Table. 2 Aerodynamic and geometrical Specification of Compressor rotor

IV RESULTS AND DISCUSSION

Figure 4 shows the performance graph of the mixed-flow impeller designed for the present work. It can be seen from the figure that maximum Total-to-static pressure ratio of impeller alone at the design mass flow parameter achievable is 3.2253 with Total-to-total isentropic efficiency of 89.76% [19].

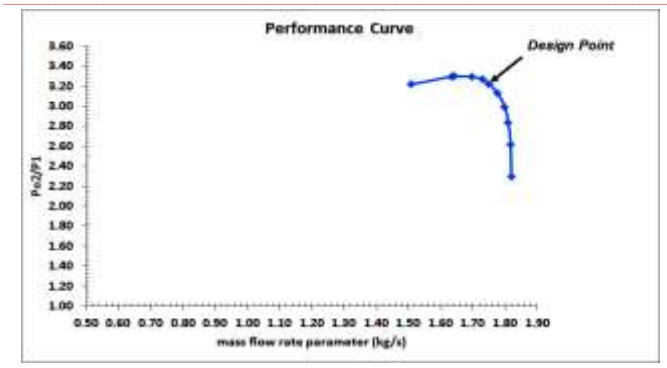

Figure 4 Total-to-static Pressure ratio vs mass flow parameter

A. Losses in the Impeller

Disc and cover friction losses (Figure-5) are rather small, except at low Reynolds number, and can be treated adequately by simple theory. In contrast, internal (Figure-6) and discharge mixing losses (Figure-7) are serious and they arise from fluid-dynamic phenomenon which is not thoroughly understood. Both types of losses strongly depend upon the relative velocity level in the impeller [1]. For maximum diffusion which we get by conversion of inlet Kinetic Energy into a static pressure rise within the impeller will ultimately results into increase in stage pressure by reducing losses. Considering the stage, we can reduce the diffuser losses also by reducing the Kinetic Energy which the diffuser must convert into a pressure rise.

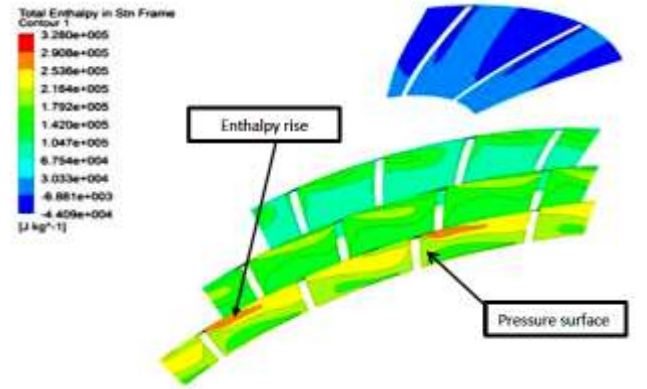

Figure 5 Disk and Cover friction

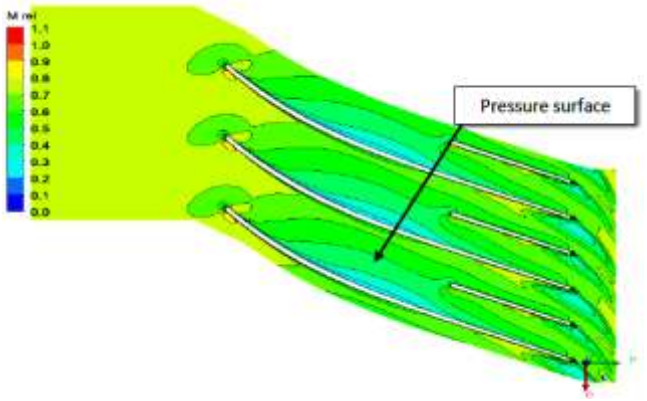

Figure. 6 Internal Flow irreversibility (Near to hub surface)

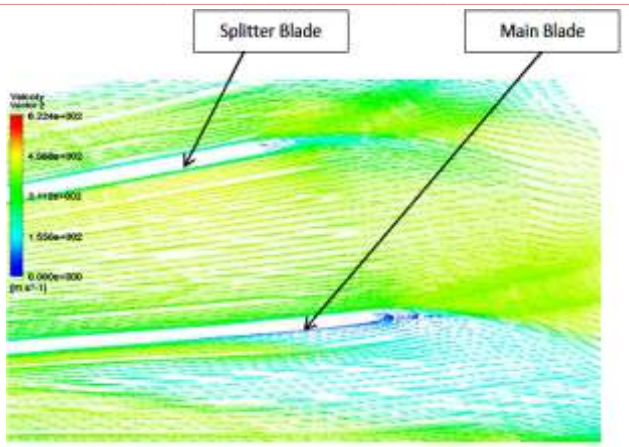

Figure 7 Discharge mixing losses (50% of the span at the trailing edge)

It can be seen from the Figure-6 that near the hub surface there is internal flow reversibility at the pressure surface of the main blade. Jet and Wake phenomenon is generally not seen in mixed-flow impellers as seen in Figure-7.

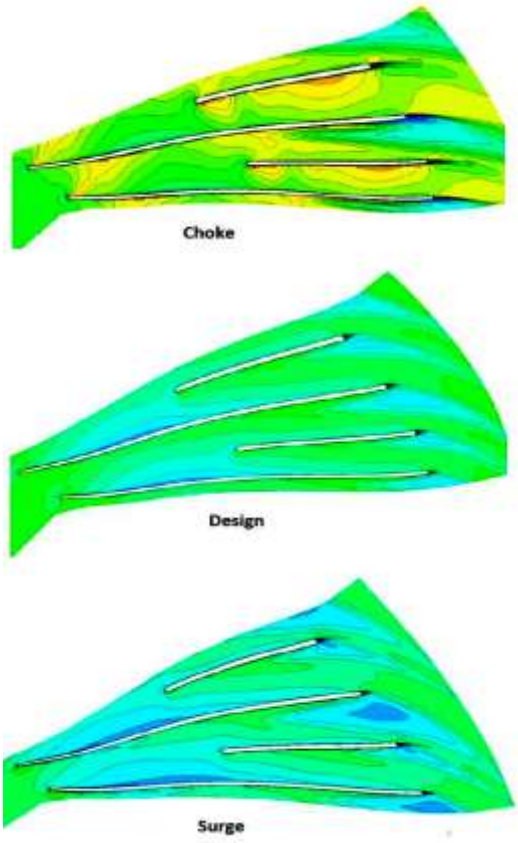

Figure 8 Relative Mach Number contour near the Hub

Relative Mach number contour near the hub region at Designed, stall and near choke condition is shown in Figure-8. It can be seen from figure that at choke point a strong shock formation is captured at leading edge pressure surface.

Figure-9 shows relative Mach number contour at mean position along the streamline. It can be seen that the strong shock on pressure surface near leading edge is captured as the result of initiation of shock near hub near to the choke condition. A trace of shock formation at suction surface near leading edge during stall mass flow rate is capture.

In Figure-10, a strong normal shock on the pressure side of the main blade is captured at choking condition due to which the flow near the suction side of the main blade is disturbed and wake region (flow reversal) has been created which results into improper growth of the flow.

Proper thickness to chord ratio (t/c) distribution from hub to tip has to be done. Increase in the thickness near the leading edge would help to properly swallow the normal shock produced near to choking condition. Flow reversal can also be avoided with proper flow path studies.

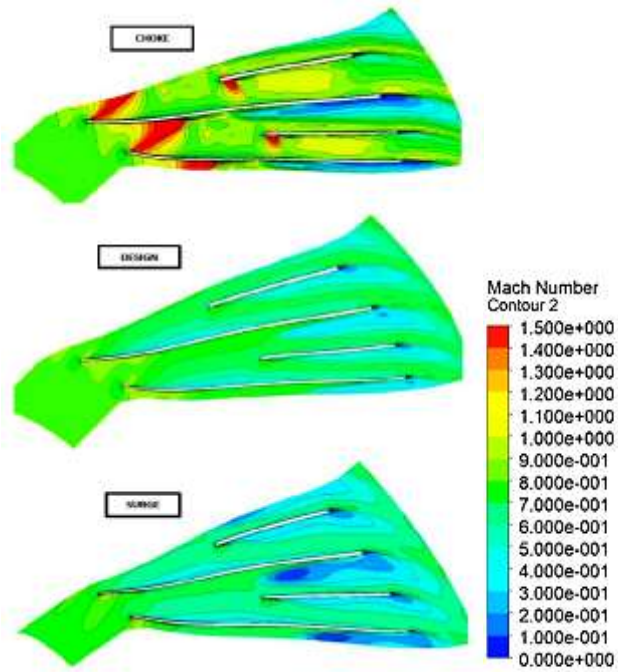

Figure 9 Relative Mach Number contour at mean along the streamline

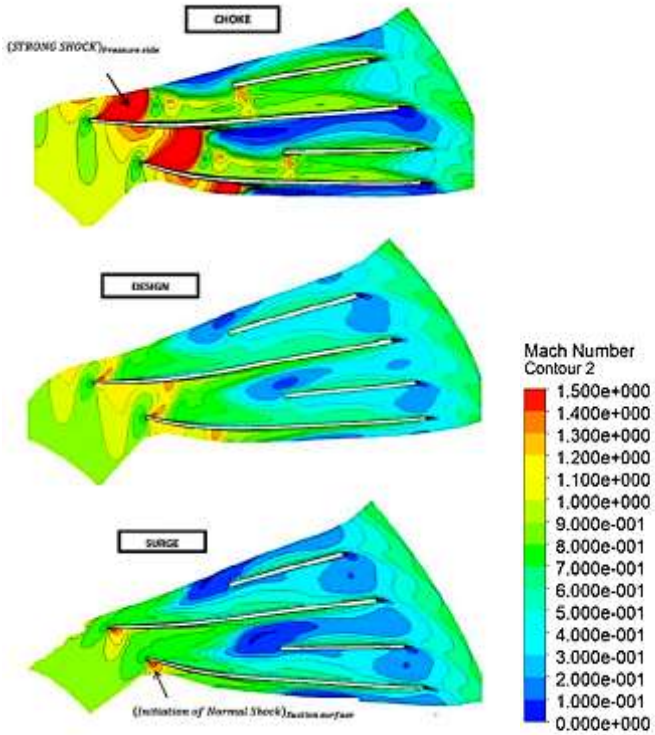

Figure 10 Relative Mach Number contour near shroud along the streamline

B. Blade Loading

Blade loading near the hub region at different mass flow rate has been captured. At design and stall mass flow rate the blade loading pattern is as usual; Blade loading of splitter blade is more at suction surface than the main blade and less at the pressure surface. But near the choke condition the blade loading is highly unstable and shows reverse trend in splitter blade than that of in other conditions. Near choke point, splitter blade have lower blade loading at suction surface than main blade and higher at pressure surface.

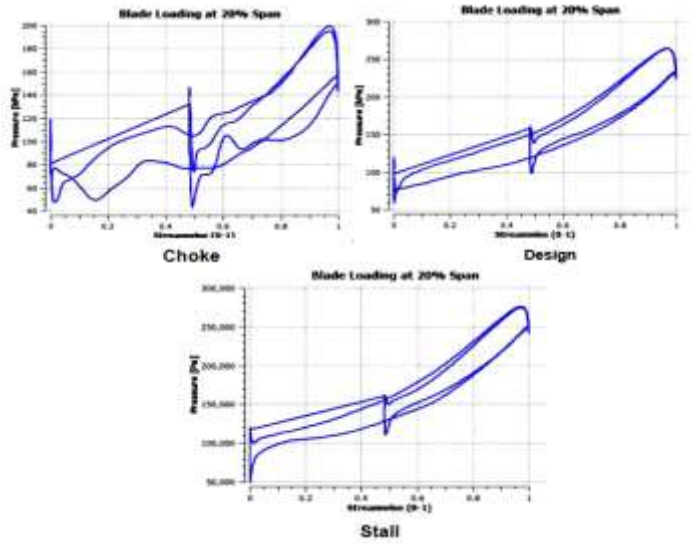

Figure 11 Blade loading near the hub at design, stall and choke mass flow rate

Figure-12 shows the velocity vector plot of the main blade and the splitter blade at mean position along the streamline. There is strong low velocity region at the trailing edge suction surface of the main blade which gradually decreases as the mass flow increases. But this low velocity zone propagates towards the leading edge which disturbs the flow over the pressure surface of the splitter blade. As the result of which a small normal shock initiation at the splitter blade suction surface leading edge can be seen.

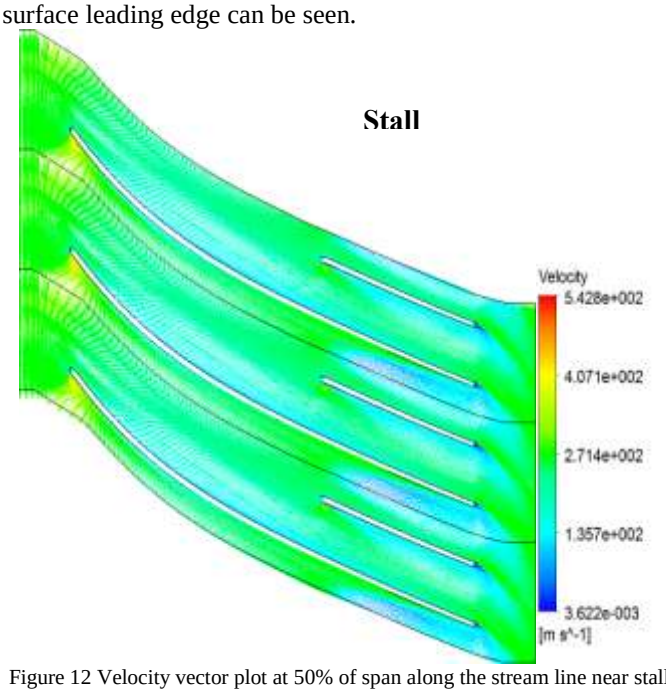

Figure 12 Velocity vector plot at 50% of span along the stream line near stall

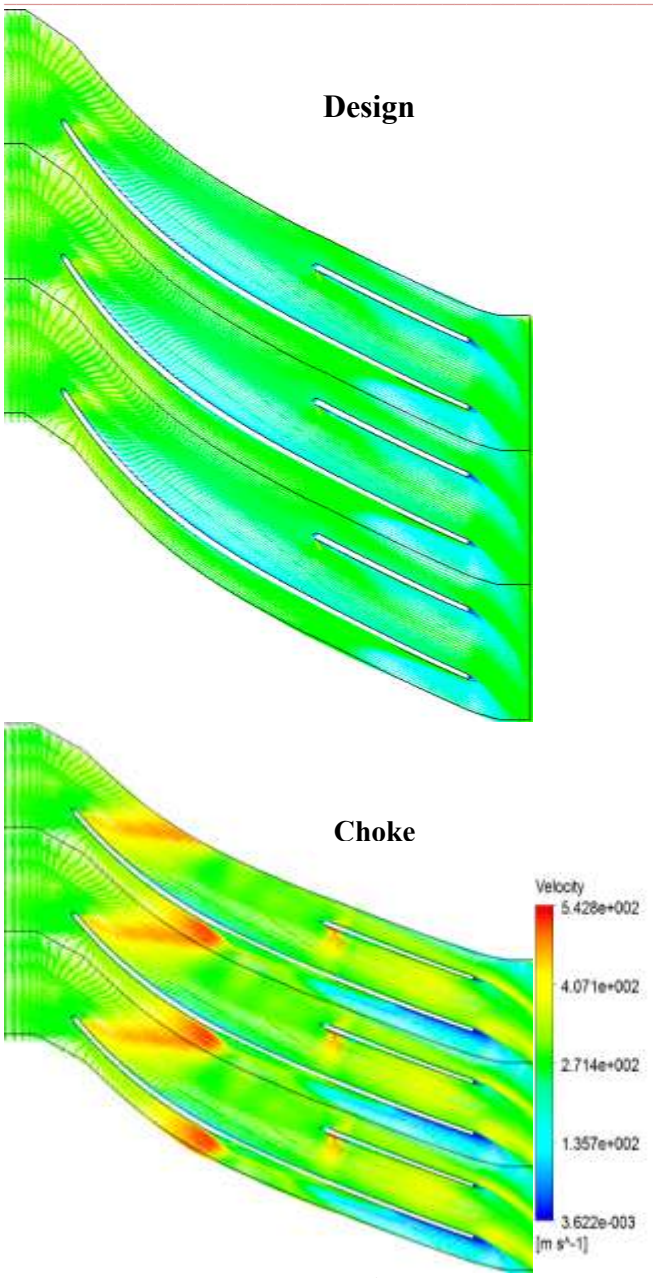

Figure 12 Velocity vector plot at 50% of span along the stream line near design and choke condition

V CONCLUSION

Increase in leading edge blade thickness near tip helps to absorb normal shock properly and may result into increase in the choke margin. Only thickness increment would not help; proper thickness to chord distribution of main blade along with suitable backsweep angle and cone angle would help to increase operating range of the impeller.

Flow reversal near the main blade pressure surface at hub region is capture which should be avoided to increase the efficiency of the impeller. Blade loading of splitter blades shows reverses behavior than the normal near the choking condition.

REFERENCES

[1] Osborne et al, "Aerodynamic and Mechanical Design
[2] of an 8:1 pressure ratio Centrifugal Compressor", Creare TN-204, June 1975, NASA-CR-134782.
[3] R. Van Den Braembusschevki, "Flow modelling and Aerodynamic design techniques for Centrifugal Compressors", Lecture series 95, 1977, von Karman Institute of Fluid Dynamics.
[4] Robert C. Dean, Jr., "The fluid dynamic design of Advanced centrifugal compressors", July 1974, Creare TN-185.
[5] S. Ramamurthy and A. M. Srharsha, " Theoretical Evaluation of Flow through a Mixed flow compressor Stage", ISABE 2009.
[6] Rajakumar et al, "CFD analysis of flow through mixed flow compressor under various operating conditions", IJSER, 2013, Vol. 4(2), ISSN 2229-5518.
[7] Seppo A. Korpela, "Principle of Turbomachinery", 2011, John Wiley & Sons, New Jersey.
[8] "The Jet Engine", Fourth Edition, 1986, Technical Publication, Rolls-Royce plc.
[9] R. Rajendran, "Flow studies in a Centrifugal compressor stage", Turbine technical conference and exhibition, ASME Turbo Expo, June-2016
[10] M. V. Herbert, "A Method of Performance Prediction for centrifugal compressors", National Gas Turbine Establishment, RM-3843, February 1980.
[11] 10. Austin King, J. and Edward, G., "Performance characteristic of Mixed-Flow Impeller and vaned diffuser with several modifications", NACA-WR-E197, July 1942.
[12] Frank J. Barina, "Comparative performance of two vaneless diffusers designed with different rates of passage curvature for Mixed-Flow Impellers", NACA-TN-1490, December 1947.
[13] Robert Anderson, J., William Ritter, K. and Dean Dildine, M., "An Investigation of the effect of Blade Curvature on Centrifugal-Impeller performance", NACA-TN-1313. May 1947.
[14] John D. Stanitz, "Two-Dimensional Compressible flow in conical Mixed-Flow Compressors", NACA-TN-1744, November 1948.
[15] Arthur W. Goldstein, "Design and Performance of experimental Axial-Discharge Mixed-Flow Compressor", NACA-RM-E8F04, August 1948
[16] Robert J. Anderson, William K. Ritter and Shirley R. Parsons, "Apparent effect of inlet temperature on adiabatic efficiency of Centrifugal Compressors", NACA-TN-1537, March 1948.
[17] Joseph T. Hamrick, Ambrose Ginsburg and Walter M. Osborn, "Method of analysis for compressible flow through Mixed-Flow Centrifugal Impellers of Arbitrary Design", NACA-TN-2165, August 1950.
[18] Joseph T. Hamrick, Walter M. Osborn, and William L. Beede, "Design and Test of Mixed-Flow Impellers III- Design and Experimental results for impeller model MF-2A and comparison with impeller model MFI-1A", NACA-RM-E52122A, March 1953.
[19] Joseph T. Hamrick, William L. Beede, and Joseph R. Withee, Jr., "Design and Test of Mixed-Flow Impellers, IV – Experimental Results for Impeller Models MF-1 and MFI-1 and MFI-2 with changes in blade height", NACA-RM-E53102, February 1954.
[20] Vishal Doshi, Emandi Rajesh, R. Rajendran, "Aero-mechanical design and analysis of a mixed-flow compressor impeller for 6:1 pressure ratio for particular geometrical constraints and specific speed", ACGT-2016, Mumbai.